

Time Resolved Collective Entanglement Dynamics in Cavity Quantum Electrodynamics

J. A. Mlynek,^{1,*} A. A. Abdumalikov Jr.,^{1,*} J. M. Fink,¹
L. Steffen,¹ M. Baur,¹ C. Lang,¹ A. F. van Loo,¹ and A. Wallraff¹

¹*Department of Physics, ETH Zürich, CH-8093, Zürich, Switzerland.*

(Dated: November 3, 2022)

Nonlinearity and entanglement are two important indications by which physical systems can be identified as non-classical. We study the dynamics of the resonant interaction of up to $N=3$ two-level systems and a single mode of the electromagnetic field. We focus on a single excitation dynamically shared in this fourpartite system. We observe coherent vacuum Rabi oscillations and their nonlinear \sqrt{N} - speed up in frequency by tracking the populations of all three qubits and the resonator. We use full quantum state tomography to verify that the dynamics generates a maximally entangled 3-qubit W-state when the cavity returns to the vacuum state.

Effects related to the interaction of light and matter can be investigated in many different physical systems. The description of this interaction can be simplified to the interplay of identical two-level systems and a single mode of an electromagnetic field. This theoretical abstraction is known as the Dicke- or Jaynes-Cummings model [1, 2]. In recent years it became feasible to investigate the complex interaction of light with multiple two-level systems as experiments approached a higher level of control over collections of individual quantum systems. The coupling strength (transition amplitude) of N two-level systems and a single mode increases as \sqrt{N} . Clear evidence of this nonlinear behavior was observed in spectroscopic measurement with few atoms [3–6], large ensembles of atoms using cold gases [7–9], ion Coulomb crystals [10] and by using superconducting qubits coupled to a transmission line resonator [11, 12].

More insight on the dynamics of collective systems can be gained by time resolved measurements of energy exchange between its individual components. When multiple two-level systems are resonantly coupled to a single mode, this process is called collective vacuum Rabi oscillations. The collective coupling strength g defines the frequency of these oscillations. Here, we restrict our investigation to the initial state in which the cavity is populated with exactly one photon. In this case the oscillation involves a single photon that is continuously absorbed and reemitted by all N two-level systems. In fact each two-level system absorbs the photon with equal probability $1/N$. Our lack of knowledge about which two-level system actually absorbs the photon leads to entangled states which are known as W-states [13]. The nonlinear enhancement of the coupling strength speeds up the generation of W-states when N is increased. The preparation of Dicke- and W-states has been demonstrated in NMR- [14], photonic- [15], ion trap- [16] and circuit QED [17] systems.

Circuit QED, in which a controllable number of superconducting qubits are strongly coupled to a single mode of a radiation field defined by a transmission line res-

onator, offers a suitable set of tools to investigate collective interactions. So far the resonant collective dynamics of a circuit QED system has been observed in time resolved measurements of two phase qubits coupled to a transmission line resonator [12]. Time resolved measurement, however, have not been carried out with more than two qubits and clear evidence of entanglement, for example by measuring the density matrix of the generated states, is still pending. Generally, the generation and observation of multi-qubit entangled states is quite challenging in these systems and was achieved only recently for up to three qubits [17–19].

Here, we report time domain studies of the collective oscillation of three fully controllable transmon-type superconducting qubits [20] coupled to a single electric field mode of a microwave resonator. The coupling of multiple two-level systems to a single mode is described by the Tavis-Cummings Hamiltonian [21]

$$\hat{\mathcal{H}}_{\text{TC}} = \hbar\omega_r \hat{a}^\dagger \hat{a} + \sum_j \left(\frac{\hbar}{2} \omega_j \hat{\sigma}_j^z + \hbar g_j (\hat{a}^\dagger \hat{\sigma}_j^- + \hat{\sigma}_j^+ \hat{a}) \right). \quad (1)$$

ω_r is the frequency of the field mode, ω_j is the transition frequency between ground state $|g\rangle$ and excited state $|e\rangle$ of the two-level system j , \hat{a} and \hat{a}^\dagger are the creation and annihilation operators of the mode and $\hat{\sigma}_j^\pm$ are the corresponding operators acting on the qubits. In our circuit QED implementation of the Hamiltonian $\hat{\mathcal{H}}_{\text{TC}}$ we use the first harmonic mode of a coplanar transmission line resonator at $\omega_r/2\pi \simeq 7.023$ GHz with quality factor $Q \simeq 14800$. An optical microscope image of the sample is shown in Fig. 1(a). The resonator is used for the resonant exchange of a single excitation and for dispersive joint three-qubit readout by measuring its transmission properties [22]. All qubits are located at the antinodes of the first harmonic mode of the resonator. The frequency of each qubit is approximately given by $\hbar\omega_j(\Phi) \approx \sqrt{8E_C E_J(\Phi)} - E_C$ where the Josephson energy depends periodically on the flux penetrating the SQUID loop according to $E_J(\phi) = E_{J\text{max}} |\cos(\pi\phi/\phi_0)|$. The maximum Josephson energies $E_J(0)/\hbar$ for the three

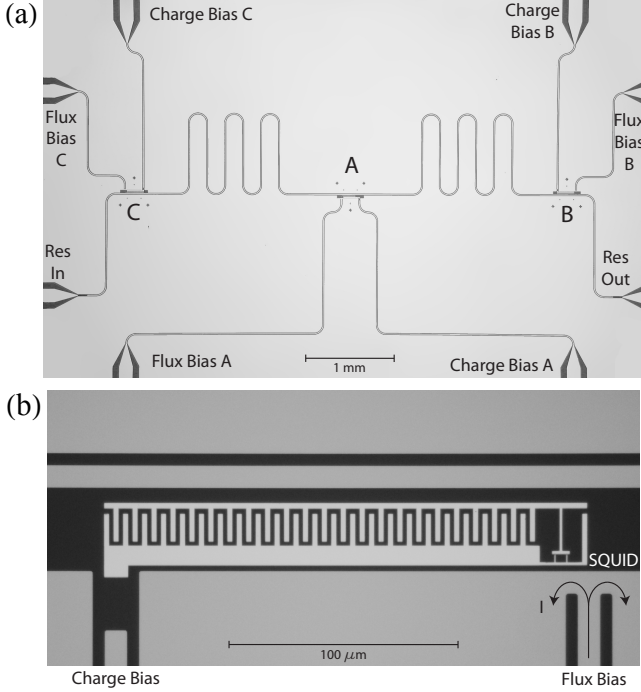


FIG. 1. (a) Optical microscope image of the sample with three qubits (A,B,C) capacitively coupled to a coplanar waveguide resonator. (b) Enlarged view of the transmon qubit C. Each qubit is equipped with individual local charge and magnetic flux-bias lines.

qubits are (26.8, 28.1, 25.7) GHz and their charging energies E_C/\hbar are (459, 359, 358) MHz. The anharmonicity of the transmon energy levels depends on E_C and is chosen such that the validity of the two-level approximation is ensured while keeping the charge dispersion low. The maximum transition frequency of the qubits $\omega_j(0)/2\pi = (9.58, 8.65, 8.23)$ GHz is designed such that all three qubits can be tuned into resonance with the resonator. In the steady state the qubits are flux biased at $\omega_j/2\pi \simeq (6.11, 4.97, 7.82)$ GHz using the quasistatic magnetic field generated by three superconducting miniature coils positioned underneath the chip, such that $|\Delta_j| \gg g_j$ with detuning $\Delta_j = \omega_j - \omega_r$. We measure qubit dephasing times $T_2 = (100, 140, 440)$ ns and qubit relaxation times $T_1 = (2.1, 1.8, 1.0)$ μ s. Tuning of the transition frequencies on the nanosecond timescale is achieved by injecting current pulses into on-chip flux control lines (see Fig. 1(b)). Both for the coils as well as for the flux gate lines we determined the full coupling matrix to compensate for cross coupling. The coupling strengths g_j of the qubits (A,B,C) extracted from spectroscopic measurements are $(g_A, g_B, g_C)/\pi = (-105.4, 110.8, 111.6)$ MHz. The negative coupling constant of qubit A originates from the π -phase difference of the first harmonic mode between the center of the resonator and its coupling ports.

By applying phase controlled truncated Gaussian

DRAG pulses [23] through the on-chip charge bias lines (see Fig. 1(b)) each qubit can be prepared in an arbitrary superposition state $\psi = \alpha|g\rangle + \beta|e\rangle$ and read out jointly [22]. The extraction of the N qubit populations needs 2^N single qubit rotations and the tomographic extraction of the full density matrix requires 2^{2N} pulses. The pulse sequence we have implemented to observe the one qubit vacuum Rabi oscillation is depicted in Fig. 2(a, left column). First, a π -pulse is applied to a single qubit far detuned from the resonator, such that the system can be described by a product state $|e\rangle \otimes |0\rangle$. Then the qubit is tuned into resonance with the resonator using a flux pulse of variable duration τ . To reduce large overshoots during resonant interaction the qubit is tuned to an intermediate buffer frequency before the final resonant pulse is applied. On resonance the energy eigenstates of this system containing $n = 1$ excitations and N qubits are $|n = 1, N = 1\pm\rangle = 1/\sqrt{2}(|g, 1\rangle \pm |e, 0\rangle)$ and the initial excited qubit state undergoes vacuum Rabi oscillations between $|g, 1\rangle$ and $|e, 0\rangle$. The frequency of the oscillations is given by $\Omega = 2\sqrt{g^2 + \Delta^2}$ with $\Omega_0 = 2g$ for $\Delta = 0$. The amplitude of the vacuum Rabi oscillation is maximal on resonance where the excitation is fully exchanged. After the resonant flux pulse of length τ the qubit is detuned from the resonator again and the energy exchange process is stopped. In addition to the dispersive readout for the qubit population we determine the resonator population by measuring the average photon number, as given by the time integrated power $\langle \hat{a}^\dagger \hat{a} \rangle$ at the output of the cavity once the oscillation is stopped [24]. As can be seen in Fig. 2(a, right column) the qubit population is oscillating with frequency of 112.0 MHz and is exactly out of phase with the photon field oscillating at an experimentally extracted frequency of 111.2 MHz. Both values are in good agreement with the spectroscopically obtained value.

We extended the procedure described above to two and three qubits as shown in the pulse diagrams in Fig. 2(b) and 2(c). We study the collective vacuum Rabi oscillations with initially a single excitation in the resonator. This initial state is prepared by transferring the full excitation of the first qubit to the resonator by adjusting the interaction time between the qubit and the resonator to $\tau_0 = \pi/2g$. Then the second and third qubit are tuned into resonance and the resonant collective interaction proceeds for time τ . All qubit populations oscillate simultaneously out of phase with the cavity. To obtain all qubit populations by a tomographic state reconstruction with a joint readout a set of single qubit rotation pulses is applied at the qubit steady state frequencies for each interaction time τ . When the number N of qubits taking part in the resonant interaction is increased, the frequency of the oscillation scales with \sqrt{N} and the amplitude of the individual qubit population decreases to $1/N$ such that normalization is fulfilled. The tripartite states between which the oscillations occur are $|g, g, 1\rangle$

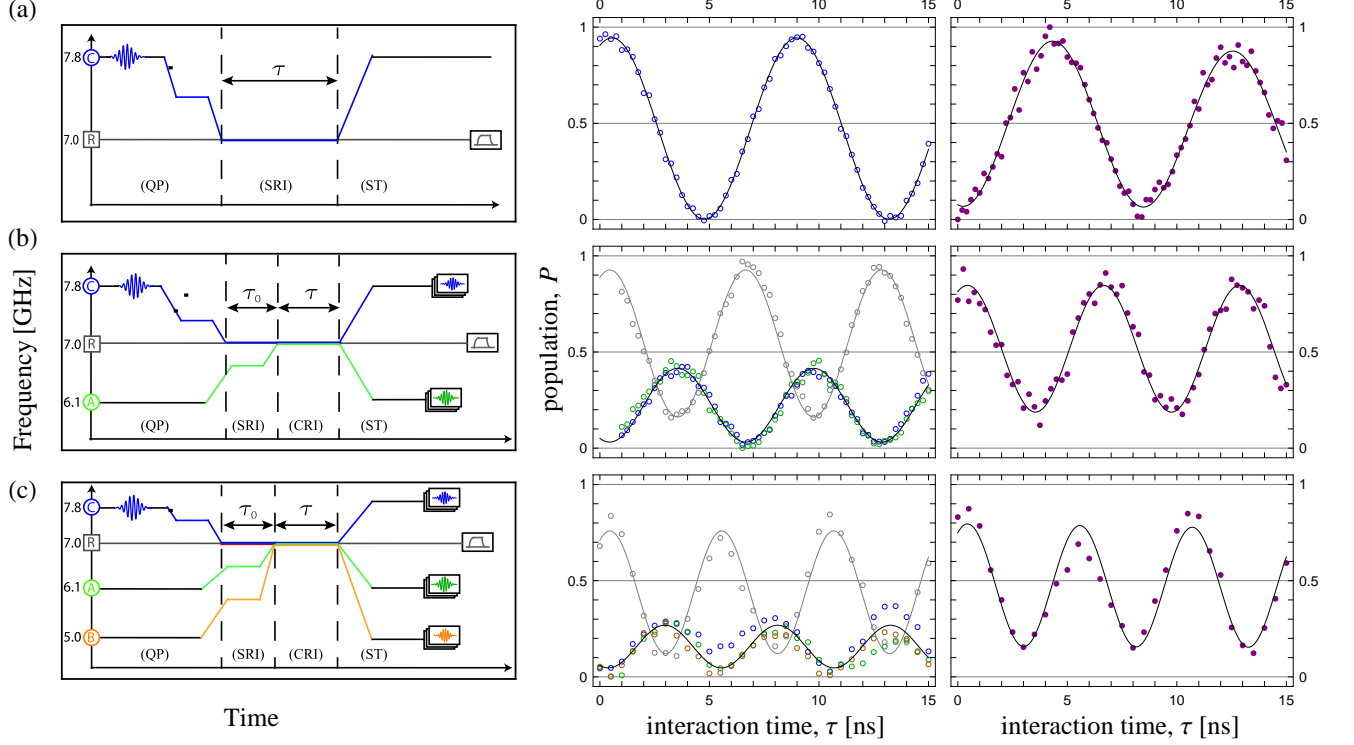


FIG. 2. Dynamics of the collective vacuum Rabi oscillations. (a) Pulse sequence for the single qubit vacuum Rabi oscillation (QP=Qubit Preparation, SRI=Single Resonant Interaction, ST=State Tomography). The population P is shown for the qubit C (blue) and the cavity (violet). (b) Pulse sequence for the two qubit collective vacuum Rabi oscillation (CRI=Collective Resonant Interaction). The population is shown for two qubits A (green) and C (blue), for the ground state (gray) and the cavity (violet). (c) Pulse sequence for the three qubit collective vacuum Rabi oscillation. The population is shown for qubit A (green), B (brown) and C (blue), for the ground state (gray) and the cavity (violet).

and $1/\sqrt{2}(|g, e, 0\rangle - |e, g, 0\rangle)$ and equivalently $|g, g, g, 1\rangle$ and $1/\sqrt{3}(|g, g, e, 0\rangle + |g, e, g, 0\rangle - |e, g, g, 0\rangle)$ for the four-partite state, where we have denoted the states in a binary order as $|C, B, A, \text{Cavity}\rangle$. The opposite phase of the $|e, g, g, 0\rangle$ state originates from the fact that qubit A has a negative coupling constant. The collective oscillation transfers energy back and forth between the qubits and the resonator, such that the population in the cavity is correlated with the population of the qubit $|ggg\rangle$ state. Hence it is instructive to measure the photonic part of the state as presented before for the single qubit vacuum Rabi oscillations (see Fig. 2(b/c, third column)).

The qubit populations measured after the collective vacuum oscillations are shown in Fig. 2(b) and Fig. 2(c, second column). The oscillation frequencies for the resonator population for $N=2$ and $N=3$ are $161.8 \text{ MHz} = 1.05 \cdot \sqrt{2} \bar{g}/2\pi$ and $195.2 \text{ MHz} = 1.03 \cdot \sqrt{3} \bar{g}/2\pi$, with \bar{g} being the root mean square [25] of the three spectroscopically obtained coupling constants. These oscillation frequencies clearly demonstrate the \sqrt{N} -nonlinearity of the Tavis-Cummings Hamiltonian in time resolved measurements. While the collective qubit oscillations are in good agreement with the expected dynamics, we ob-

serve a decrease in visibility with increasing N for both the qubit and resonator populations. We attribute this observation to an imperfect control of the flux pulse amplitudes. Although we extracted a flux pulse cross coupling matrix, its accuracy is not sufficient to fully compensate the flux cross talk and to exactly tune all qubits into resonance with the resonator. During the collective oscillations the W-state is created at time $\tau = \pi/(2\bar{g}\sqrt{N})$, i.e. when the cavity state factorizes $|0\rangle \otimes 1/\sqrt{3}(|g, g, e\rangle + |g, e, g\rangle - |e, g, g\rangle)$. We measured the three qubit density matrix at this time by applying full quantum state tomography [22]. The result is shown in Fig. 3(a) and was obtained by applying the pulse sequence shown in figure 2(c). All three qubits were tuned out of resonance after only $\tau = 2.9 \text{ ns}$ of collective interaction. If needed the dynamic phase that is picked up during the time when the qubits are detuned can be corrected by applying single qubit phase gates or by adjusting the phases of the tomography pulses. Here the coherent entries of the density matrix have been numerically rotated to correspond to the phases in the expected state. This allowed us to characterize the measured state by defining the fidelity as $\langle \rho_t | \rho_{ppm} | \rho_t \rangle$ with ρ_{ppm} be-

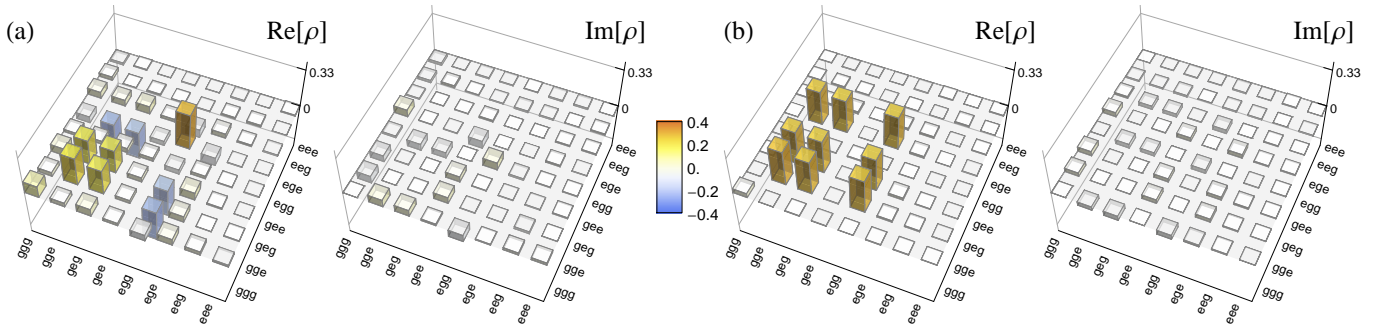


FIG. 3. Measured density matrix of the W-state. (a) Obtained for the collective approach as shown in figure 2. (b) Generated by the sequential approach.

ing the rotated density matrix. After applying a maximum likelihood estimation [26] the resulting fidelity is 78 % with respect to the density matrix $\rho_t = |\Psi_W\rangle\langle\Psi_W|$ and $\Psi_W = 1/\sqrt{3}(|g, g, e\rangle + |g, e, g\rangle - |e, g, g\rangle)$ being the ideal state. As already discussed in the context of time resolved measurements the dominant limitation to our control over the oscillation is flux cross talk.

For comparison we have also prepared the W-state using a sequential method. Also in this approach we distribute a single excitation equally between the three qubits using resonant interaction. First, we excite qubit C and tune it into resonance with the resonator for time $\tau_1 = \arcsin(\sqrt{2/3})/g_C$. During this interaction, only 2/3 of the energy is transferred to the resonator. Next we tune qubit B into resonance for a time $\tau_2 = \arcsin(\sqrt{1/2})/g_B$, transferring half of the resonator energy to qubit B. Finally we let qubit A pick up the remaining third of the energy from the resonator by bringing it into resonance for a time $\tau_3 = \arcsin(1)/g_A$. Using a joint readout and tomography we obtain a density matrix of the W-state with fidelity 91%.

As expected the preparation time for the consecutive attempt is indeed longer than for the collective approach, because the latter method exploits the \sqrt{N} -enhancement. The fact that the higher fidelity was obtained by a procedure where no flux pulses are injected simultaneously affirms that the main limitation of the collective generation is due to residual flux crosstalk rather than decoherence.

In summary, we have experimentally studied collective vacuum Rabi oscillations of three superconducting qubits coupled to a microwave resonator. We have fully resolved the dynamics of the population in the time domain. The \sqrt{N} -scaling of the oscillation frequency of the collective vacuum Rabi oscillations and the generation of multi-qubit entanglement were studied. Moreover we compared the collective method to an approach that achieves entanglement sequentially. The techniques used and developed allowed for the complete examination of collective effects by taking advantage of individual control over all involved system components.

This work was supported by the Swiss National Science Foundation (SNF) and the EU IP SOLID.

* These authors contributed equally to this work.

- [1] R. H. Dicke, Phys. Rev. **93**, 99 (1954).
- [2] E. Jaynes and F. Cummings, Proceedings of the IEEE **51**, 89 (1963).
- [3] F. Bernardot, P. Nussenzveig, M. Brune, J. M. Raimond, and S. Haroche, Europhys. Lett. **17**, 33 (1992).
- [4] J. J. Childs, K. An, M. S. Otteson, R. R. Dasari, and M. S. Feld, Phys. Rev. Lett. **77**, 2901 (1996).
- [5] R. J. Thompson, Q. A. Turchette, O. Carnal, and H. J. Kimble, Phys. Rev. A **57**, 3084 (1998).
- [6] P. Münstermann, T. Fischer, P. Maunz, P. W. H. Pinkse, and G. Rempe, Phys. Rev. Lett. **84**, 4068 (2000).
- [7] F. Brennecke, T. Donner, S. Ritter, T. Bourdel, M. Kohl, and T. Esslinger, Nature **450**, 268 (2007).
- [8] Y. Colombe, T. Steinmetz, G. Dubois, F. Linke, D. Hunger, and J. Reichel, Nature **450**, 272 (2007).
- [9] A. K. Tuchman, R. Long, G. Vrijsen, J. Boudet, J. Lee, and M. A. Kasevich, Phys. Rev. A **74**, 053821 (2006).
- [10] P. F. Herskind, A. Dantan, J. P. Marler, M. Albert, and M. Drewsen, Nat. Phys. **5**, 494 (2009).
- [11] J. M. Fink, R. Bianchetti, M. Baur, M. Goppl, L. Steffen, S. Filipp, P. J. Leek, A. Blais, and A. Wallraff, Phys. Rev. Lett. **103**, 083601 (2009).
- [12] F. Altomare, J. I. Park, K. Cicak, M. A. Sillanpää, M. S. Allman, D. Li, A. Sirois, J. A. Strong, W. J. D., and R. W. Simmonds, Nat. Phys. **6**, 777 (2010).
- [13] W. Dür, G. Vidal, and J. I. Cirac, Phys. Rev. A **62**, 062314 (2000).
- [14] G. Teklemariam, E. M. Fortunato, M. A. Pravia, Y. Sharf, T. F. Havel, D. G. Cory, A. Bhattaharyya, and J. Hou, Phys. Rev. A **66**, 012309 (2002).
- [15] M. Eibl, N. Kiesel, M. Bourennane, C. Kurtsiefer, and H. Weinfurter, Phys. Rev. Lett. **92**, 077901 (2004).
- [16] C. F. Roos, M. Riebe, H. Haffner, W. Hansel, J. Benhelm, G. P. T. Lancaster, C. Becher, F. Schmidt-Kaler, and R. Blatt, Science **304**, 1478 (2004).
- [17] M. Neeley, R. C. Bialczak, M. Lenander, E. Lucero, M. Mariantoni, A. D. O'Connell, D. Sank, H. Wang, M. Weides, J. Wenner, Y. Yin, T. Yamamoto, A. N. Cleland, and J. M. Martinis, Nature **467**, 570 (2010).

- [18] L. DiCarlo, M. D. Reed, L. Sun, B. R. Johnson, J. M. Chow, J. M. Gambetta, L. Frunzio, S. M. Girvin, M. H. Devoret, and S. R. J., *Nature* **467**, 574 (2010).
- [19] M. Baur, A. Fedorov, L. Steffen, S. Filipp, M. P. da Silva, and A. Wallraff, *Phys. Rev. Lett.* **108**, 040502 (2012).
- [20] J. Koch, T. M. Yu, J. Gambetta, A. A. Houck, D. I. Schuster, J. Majer, A. Blais, M. H. Devoret, S. M. Girvin, and R. J. Schoelkopf, *Phys. Rev. A* **76**, 042319 (2007).
- [21] M. Tavis and F. W. Cummings, *Phys. Rev.* **170**, 379 (1968).
- [22] S. Filipp, P. Maurer, P. J. Leek, M. Baur, R. Bianchetti, J. M. Fink, M. Göppl, L. Steffen, J. M. Gambetta, A. Blais, and A. Wallraff, *Phys. Rev. Lett.* **102**, 200402 (2009).
- [23] J. M. Gambetta, F. Motzoi, S. T. Merkel, and F. K. Wilhelm, *Phys. Rev. A* **83**, 012308 (2011).
- [24] D. Bozyigit, C. Lang, L. Steffen, J. M. Fink, C. Eichler, M. Baur, R. Bianchetti, P. J. Leek, S. Filipp, M. P. da Silva, A. Blais, and A. Wallraff, *Nat. Phys.* **7**, 154 (2011).
- [25] C. E. López, H. Christ, J. C. Retamal, and E. Solano, *Phys. Rev. A* **75**, 033818 (2007).
- [26] J. A. Smolin, J. M. Gambetta, and G. Smith, *Phys. Rev. Lett.* **108**, 070502 (2012).